Characterization of the Structural, Optical, and Dielectric Properties of Oxynitride Perovskites AMO_2N (A = Ba, Sr, Ca; M = Ta, Nb)

Young-Il Kim,[†] Patrick M. Woodward,*[,†] Karim Z. Baba-Kishi,[‡] and Cheuk W. Tai[‡]

Department of Chemistry, The Ohio State University, Columbus, Ohio 43210, and Department of Applied Physics, The Hong Kong Polytechnic University, Hung Hom, Kowloon, Hong Kong

Received August 15, 2003. Revised Manuscript Received January 26, 2004

The syntheses, crystal structures, electrical properties, and optical absorbance spectra of six perovskite oxynitrides, AMO_2N (A = Ba, Sr, Ca; M = Ta, Nb) have been investigated. The average crystal structure of $BaTaO_2N$ is a cubic perovskite, with a Ta−O/N distance of 2.056 Å. $SrTaO_2N$ and $CaTaO_2N$ are distorted by octahedral tilting, showing noticeably smaller Ta−O/N distances of approximately 2.02 Å. Electron diffraction studies of $BaTaO_2N$ are consistent with the simple cubic perovskite crystal structure determined using X-ray powder diffraction methods. Each of the niobium oxynitrides is isostructural with its tantalum analogue, though the Nb−O/N distances are observed to be slightly longer. The optical band gaps are estimated from diffuse reflectance spectra as follows: $BaTaO_2N$, 1.8 eV; $SrTaO_2N$, 2.1 eV; $CaTaO_2N$, 2.4 eV; $BaNbO_2N$, 1.8 eV; $SrNbO_2N$, 1.9 eV; $CaNbO_2N$, 2.1 eV. Impedance spectroscopy was carried out on sintered pellets of the $ATaO_2N$ and $BaNbO_2N$ to investigate the dielectric and electrical transport properties. The $BaNbO_2N$ sample shows metallic-type conductivity apparently from a slight reduction that occurs during sintering. In contrast, the tantalum compounds are semiconductors/insulators with conductivities of $\sim 10^{-5}$ S/cm (A = Ba, Sr) and $\sim 10^{-8}$ S/cm (A = Ca). Interpretation of the impedance data for $BaTaO_2N$ and $SrTaO_2N$ reveals that these two compounds have unexpectedly high bulk dielectric constants, $\kappa \approx 4900$ and 2900, respectively, at room temperature. The dielectric constants of both compounds are frequency dependent and show a relatively weak linear dependence upon temperature with no sign of a phase transition over the temperature range 300−180 K.

Introduction

Dielectric materials have the ability to store electrical energy. These materials are utilized as capacitors, resonators, switches, etc. in virtually all electricity-driven devices.[1,2] High dielectric constant (κ) and low dielectric loss ($\tan \delta$) are important criteria for designing miniaturized and elegant devices,[3] but it is no less important that the manufactured components exhibit constant fidelity over a wide range of operational conditions.[4] Despite extensive studies in the past, there is still much to be done to simultaneously achieve high κ (>1,000) and low temperature coefficient (<100 ppm/K) in a dielectric material. This is due to the fact that the dielectric permittivity changes rapidly as a function of temperature as the Curie temperature is approached. This property of normal ferroelectrics can seriously limit the useful temperature range of these materials in devices. In this context, a class of dielectric materials, referred to as relaxor ferroelectrics or simply relaxors, has been developed in complex perovskites with the general formula of $Pb(M_xM'_{1-x})O_3$.[5] They maintain high κ over a broad temperature range. The underlying principle behind the behavior of relaxors is that the phase transitions are smeared out over a wide range of temperatures due to compositional heterogeneity on the nanometer length scale. The heterogeneity arises from disorder in the octahedral cation distribution.[6]

Recently, oxynitride perovskites and related phases have received considerable attention owing to their potential applicability for nontoxic inorganic pigments and photocatalysts.[7−9] It is understood that the partial replacement of O^{-2} by N^{-3} narrows the band gap of the parent oxide by shifting its valence band edge upward.

* To whom correspondence should be addressed. Phone: 1-614-688-8274. Fax: 1-614-292-1362. E-mail: woodward@chemistry.ohio-state.edu.

[†] The Ohio State University.

[‡] The Hong Kong Polytechnic University.

(1) Davies, P. K.; Roth, R. S. *Chemistry of Electronic Ceramic Materials*; National Institute of Standards and Technology Special Publication 804; NIST: Gaithersburg, MD, 1991.

(2) Lines, M. E.; Glass, A. M. *Principles and Applications of Ferroelectrics and Related Materials*; Oxford: New York, 1997.

(3) Reaney, I. M.; Ubic, R. *Int. Ceram.* **2000**, *1*, 43.

(4) Colla, E. L.; Reaney, I. M.; Setter, N. *J. Appl. Phys.* **1993**, *74*, 3414.

(5) Cross, L. E. *Ferroelectrics* **1987**, *76*, 241.

(6) (a) Smolenskii, G. A.; Agranovskaya, A. I. *Soviet Phys. Solid State* **1959**, *1*, 1959. (b) Smolenskii, G. A. *J. Phys. Soc. Jpn.* **1970**, *S28*, 26.

(7) Jansen, M.; Letschert, H. P. *Nature* **2002**, *404*, 980.

(8) Kasahara, A.; Nukumizu, K.; Hitoki, G.; Takata, T.; Kondo, J. N.; Hara, M.; Kobayashi, H.; Domen, K. *J. Phys. Chem. A* **2002**, *106*, 6750.

(9) Hitoki, G.; Takata, T.; Kondo, J. N.; Hara, M.; Kobayashi, H.; Domen, K. *Chem. Commun.* **2002**, 1698.

10.1021/cm034756j CCC: $27.50
Published on Web 03/09/2004

The change in the resulting optical properties has fueled a number of recent studies. However, the changes in bonding and structure that accompany the introduction of nitride ions may also give rise to interesting dielectric behavior. Oxynitrides can often be described as derivatives of oxides, formed by simultaneous substitutions of cation and anion components. For example, simultaneous substitution on the Ti^{4+} and O^{-2} sites converts the oxide $SrTiO_3$ to the oxynitride $SrTaO_2N$. This type of aliovalent substitution provides a mechanism for enhancing the dielectric polarizability through the substitution of more polarizable ions into the lattice.[10] Furthermore, the reduced electronegativity of the nitride ion, with respect to the oxide ion, will tend to increase the covalency of the cation−anion bonds. The increased covalency of the bonding can in turn increase the likelihood of cation displacements through a second-order Jahn−Teller distortion of the d^0 cation.[11] It is well-known that such displacements are the origin of ferroelectricity. On the other hand, the mixed occupancy of the anion site in oxynitrides, $AM(O_{1-x}N_x)_3$, provides a condition similar to that found in relaxors, as the polarizing octahedral cations will experience random chemical environments in the absence of complete O/N ordering. It is therefore, an interesting matter to examine whether the oxynitride perovskites possess intrinsically high κ and relaxor-like properties. Previously, Marchand et al. proposed that utilization of oxynitride dielectrics would have merit because the oxynitrides, stable in reducing atmosphere, could be fabricated with low-cost nonjewelry metal electrodes. However, relatively little work has resulted from this proposal.[12,13] Herein, we report the dielectric properties and electrical conductivities of four oxynitride perovskites, $BaTaO_2N$, $SrTaO_2N$, $CaTaO_2N$, and $BaNbO_2N$, examined by impedance spectroscopy.

Experimental Section

Perovskite oxynitride samples, AMO_2N (A = Ba, Sr, Ca; M = Ta, Nb) were prepared by ammonolysis reaction[14] using $BaCO_3$ (J. T. Baker, 99.8%), $SrCO_3$ (Aldrich, 99.9+ %), $CaCO_3$ (Mallinckrodt, 99.95%), Ta_2O_5 (Cerac, 99.5%), and Nb_2O_5 (Alfa, 99.9%). A stoichiometric mixture (with respect to the cation stoichiometry) of reagents was mixed in acetone using an agate mortar and pestle, placed in an alumina boat, and heated in flowing anhydrous ammonia (99.99%, ∼0.5 mL/sec). For each composition, ∼1 g of the starting material was heated at a rate of 5 K/min to the target temperature, then held at that temperature for 20 h before cooling back to room temperature at a rate of 10 K/min. Because the progress of ammonolysis depends critically on the diffusivity of NH_3 into oxide grains, the reactants were always heated in powdered form. When starting materials were prepared in the form of a pressed pellet, swelling and/or color gradients were observed after heating in NH_3. Samples with A = Ba and Sr could be obtained at 1223−1273 K with total dwell times less than 80 h, but the Ca analogues were not readily formed in single phase form because of the stability of competing phases. In the reaction aimed at producing $CaTaO_2N$, the pyrochlore phase $Ca_2Ta_2O_7$ was formed as minor impurity phase in the early stages of the reaction and persisted even after 240 h at 1373 K. To accelerate the nitridation of $Ca_2Ta_2O_7$ into $CaTaO_2N$, the intermediate phase was reacted in a 50:50 wt % NaCl/KCl flux. This procedure significantly shortened the reaction time to ∼80 h. The synthesis of $CaNbO_2N$ was complicated by the occurrence of a niobium oxynitride phase, NbO_xN_y,[15] which occurred in equilibrium with the desired perovskite phase over a wide temperature range, 1023−1373 K. Once formed, NbO_xN_y did not decompose under the NH_3 atmosphere. Consequently, the synthesis temperature for $CaNbO_2N$ had to be kept below 1023 K. Apparently, the constituent Ca^{2+}, Nb^{5+}, O^{-2}, and N^{-3} ions do not possess sufficient diffusivity to form a single-phase sample at such low temperatures, and use of the aforementioned NaCl/KCl mineralizers effectively lowers the activation barrier for forming the perovskite phase. Starting from the ternary oxide, $Ca_2Nb_2O_7$, rather than a mixture of $CaCO_3$ and Nb_2O_5, helped to minimize formation of NbO_xN_y. With the aid of salt additives, $CaNbO_2N$ was obtained from the ammonolysis of $Ca_2Nb_2O_7$ at 1003 K for 80 h. Final phase-pure oxynitrides exhibited various chromatic colors of red-brown ($BaTaO_2N$), orange-red ($SrTaO_2N$), yellow ($CaTaO_2N$), black-brown ($BaNbO_2N$), dull brown ($SrNbO_2N$), and ocher ($CaNbO_2N$).

Phase purity was monitored using X-ray powder diffraction (XRPD) and UV−Visible diffuse reflectance spectroscopy. XRPD patterns were measured in the Bragg−Brentano reflection geometry on a Bruker D8 diffractometer equipped with an incident beam Ge 111 monochromator, which selects only Cu $K\alpha_1$ radiation (λ = 1.5406 Å), and a Braun linear position sensitive detector. The data were collected over the angular range $20° < 2\theta < 120°$ with a step size of 0.014265° and counting times of 2−4 sec per step. To minimize possible complications due to preferred orientation, samples were sprinkled through a 100-mesh sieve onto a sample holder coated with petroleum jelly. Structures were refined using the Rietveld method as incorporated in the GSAS software suite.[16]

UV−Visible diffuse reflectance data were collected and converted to absorbance using a Perkin-Elmer Lambda 20 scanning double-beam spectrometer equipped with a 50-mm Labsphere integrating sphere over the spectral range 200−1100 nm (6.2−1.1 eV). The band gap energies quoted in this study were determined from Shapiro's method[17] of extrapolating the onset of absorption to the wavelength axis.

To determine the anion stoichiometry, combustion analysis (Midwest Microanalysis, Indianapolis, IN) was employed together with thermogravimetric analysis (TGA) up to 1423 K (heating rate, 5 K/min) in flowing O_2 (40 mL/min) in a Perkin-Elmer thermal analyzer (TA7). Together with the nitrogen mass fraction directly taken from the combustion analysis, the mass change during the TGA was used as complementary information to determine the stoichiometry.

Various grains of $BaTaO_2N$ were investigated in the transmission electron microscope (TEM) to obtain diffraction patterns and determine the presence of possible distortions from cubic symmetry. The sample studied was in the powder form, cold-pressed into a disk, and comprised of crystallites about a few hundred nanometers in size. For the TEM study, a sample was imbedded in clear resin, ground and polished to a thickness of ∼30 μm, and subsequently transferred onto a TEM supporting copper grid. Ion milling was performed with argon ions at 5 kV. The studies were carried out on a JEOL-2011 microscope at 200 kV.

The dielectric permittivity and electrical conductivity of $ATaO_2N$ (A = Ba, Sr, Ca) and $BaNbO_2N$ were studied using a commercial impedance analyzer (Solartron SI1260) over the temperature range 180−300 K. Compact pellet samples were prepared by the stepwise process of uniaxial pressing (30 kpsi) of the powdered oxynitride samples, followed by cold isostatic pressing (60 kpsi, American Isostatic Presses Inc., Columbus,

(10) Shannon, R. D. *J. Appl. Phys.* **1993**, *73*, 348.
(11) (a) Halasyamani, P. S.; Poeppelmeier, K. R. *Chem. Mater.* **1998**, *10*, 2753. (b) Bersuker, I. B. *Chem. Rev.* **2001**, *101*, 1067. (c) Burdett, J. K. *Chemical Bonding in Solids*; Oxford: New York, 1995.
(12) Marchand, R.; Laurent, Y. *U.S. Patent* 4734390, 1998.
(13) Marchand, R.; Pors, F.; Laurent, Y.; Regreny, O.; Lostec, J.; Haussonne, J. M. *J. Phys.* **1986**, *C1*, C1−901.
(14) Marchand, R.; Laurent, Y.; Guyader, J.; L'Haridon, P.; Verdier, P. *J. Eur. Ceram. Soc.* **1991**, *8*, 197.
(15) Schwartz, V.; Oyama, S. T. *Chem. Mater.* **1997**, *9*, 3052.
(16) Larson, A. C.; von Dreele, R. B. *General Structure Analysis System*; Los Alamos National Laboratory Report LAUR 86-748; 1994.
(17) Shapiro, I. P. *Opt. Spektrosk.* **1958**, *4*, 256.

OH), and heating under flowing NH_3 at 1293 K for 2 h. The sintering process is critical to obtain meaningful measurements of the dielectric permittivity and conductivity, but it was not uniformly successful for all samples. This point is discussed in greater detail in the results section. Finally, to form the electrode contacts, a Ga−In eutectic (Alfa, 99.99%, Ga/In 75.5:24.5 wt %) was first rubbed on both faces of the pellets, which were then covered with Ag paste. The electrode area and sample thickness were measured in each case, and observed to fall in the range of 0.05∼0.1 cm^2 and ∼0.08 cm, respectively. The impedance spectra, measured at $1-10^7$ Hz, were interpreted by equivalent circuit analysis,[18] where κ and σ_{el} of bulk and grain boundary components were evaluated from the fitting parameters, resistance (R) and capacitance (C).[19]

Results

Compositional Analysis. First of all we attempted to ascertain whether the sample stoichiometries were AMO_2N as intended. Combustion analysis provides the weight fraction of nitrogen in sample. In the course of thermogravimetric analysis (TGA) up to 1423 K in an atmosphere containing oxygen (i.e., air), it is expected that the nitride ions in the oxynitrides will be lost and $A_2M_2O_7$ oxide phases will be formed according to the following reaction: $4AMO_2N(s) + 3O_2(g) \rightarrow 2A_2M_2O_7(s) + 2N_2(g)$. Complete oxidation during TGA was confirmed by XRPD measurements on the resulting white powders. If we combine the TGA mass increase with the nitrogen content obtained from combustion analysis, it is possible to obtain a numerical estimate of the stoichiometry. The results of this analysis are $(BaTa)_{0.97}O_{2.05}N_{0.95}$, $(SrTa)_{0.96}O_{1.91}N_{1.09}$, $(CaTa)_{0.96}O_{1.97}N_{1.03}$, $(BaNb)_{0.96}O_{2.02}N_{0.98}$, $(SrNb)_{0.98}O_{1.97}N_{1.03}$ and $(CaNb)_{0.95}O_{2.08}N_{0.92}$. Within the errors of the combustion analysis, the O:N ratio seems to be consistently 2:1, but the TGA weight gain implies the possible existence of $(AM)_{1-\delta}X_3$ ($0.02 < \delta < 0.05$) type nonstoichiometry. However, a defect model based on cation vacancies is an unrealistic model, because the cation oxidation states will not allow it. A more likely explanation for the deviation between nominal and measured stoichiometry is the possible presence of anionic species such as OH^- or perhaps NH^{-2} (these would permit the presence of cation vacancies) along with some adsorbed water. We note that our crystallographic unit cell volumes are in very good agreement with previous reports on these compounds, as are the observed colors. Thus, there is strong evidence that we are making the same oxynitride phases as those reported by others, and in fact the stoichiometry may be exactly as intended. However, it is possible that the stoichiometry and anion population are somewhat more complex than typically assumed.

UV−Visible Diffuse Reflectance Spectroscopy. The diffuse reflectance spectra of the six compounds under study are shown in Figure 1. In previous reports, optical properties of these oxynitrides have mostly been limited to a simple description of the color. However, a recent colorimetric study on $Ca_{1-x}La_xTaO_{2-x}N_{1+x}$ (x = 0.05−1.00)[7] showed that the $Ca_{0.95}La_{0.05}TaO_{1.95}N_{1.05}$ composition has an absorption that begins at 2.75 eV (∼450 nm) and exhibits a bright yellow color, close to that of commercial cadmium yellow (CdS). Our measured value for the band gap of $CaTaO_2N$ is smaller, at ∼2.4 eV. The difference between the two reports is not clear. It likely stems from the different methods that are used to obtain a numerical estimate of band gap. It is worthwhile to point out that in the semiconductor literature CdS is reported to have a band gap of 2.42 eV, very close to the value we ascribe to $CaTaO_2N$.[20] The smaller band gaps of the niobium compounds with respect to their tantalum analogues can be traced to the fact that Nb^{5+} is more electronegative than Ta^{5+}. In oxide perovskites the difference in electronegativity between these two seemingly similar ions has been called upon to explain the observation that niobium-containing compounds consistently have smaller band gaps than isostructural compounds containing tantalum.[21] By extension the optical trends also imply that the more electronegative niobium will form a more covalent interaction with the anions.

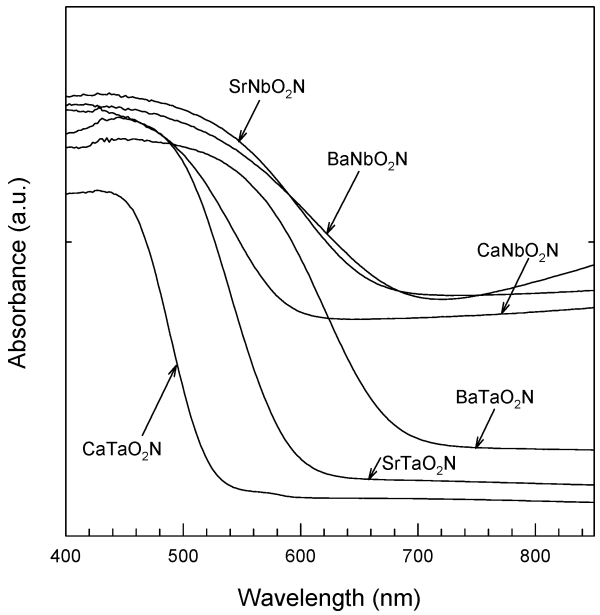

Figure 1. Diffuse reflection−absorption spectra for AMO_2N (A = Ba, Sr, Ca; M = Ta, Nb).

Room-Temperature X-ray Powder Diffraction. The crystal structures of $BaTaO_2N$,[22a] $BaNbO_2N$,[22a] $SrTaO_2N$,[22b,23] and $CaTaO_2N$[22b] have previously been determined from neutron powder diffraction data, whereas detailed structural data for $SrNbO_2N$ and $CaNbO_2N$ have not been reported in the literature. To confirm the structure and composition of our samples and to structurally characterize the latter two compounds we refined the structures of these six phases using monochromatic laboratory XRPD data. A sum-

(18) Macdonald, J. R. *Impedance Spectroscopy*; John Wiley & Sons: New York, 1987.

(19) $\kappa = Ct/(\epsilon_0 A)$ and $\sigma_{el} = t/(RA)$, where t is distance between electrodes, A is area of electrode, and ϵ_0 is permittivity of vacuum, 8.854×10^{-14} F/cm. Impedance of constant phase element is mathematically expressed as $Z_{CPE} = Z' + jZ'' = C^{-1}(j\omega)^{-p}$, where j is $\sqrt{-1}$, ω ($= 2\pi f$) angular frequency, and p accounts for the distributed time constants of relaxation.

(20) Wolfe, C. M.; Holonyak, N., Jr.; Stillman, G. E. *Physical Properties of Semiconductors*; Prentice Hall: Englewood Cliffs, NJ, 1989.

(21) Eng, H. W.; Barnes, P. W.; Auer, B. M.; Woodward, P. M. *J. Solid State Chem.* **2003**, *96*, 535.

(22) (a) Pors, F.; Marchand, R.; Laurent, Y.; Batcher, P.; Roult, G. *Mater. Res. Bull.* **1988**, *23*, 1447. (b) Gunther, E.; Hagenmayer, R.; Jansen, M. *Z. Anorg. Allg. Chem.* **2000**, *626*, 1519.

(23) Clarke, S. J.; Hardstone, K. A.; Michie, C. W.; Rosseinsky, M. J. *Chem. Mater.* **2002**, *14*, 2664.

Table 1. Summary of Structure Refinements Using XRPD Patterns for Perovskite Oxynitrides, AMO_2N (A = Ba, Sr, Ca; M = Ta, Nb)

	$BaTaO_2N$	$SrTaO_2N$	$CaTaO_2N$	$BaNbO_2N$	$SrNbO_2N$	$CaNbO_2N$
space group	*Pm*3*m*	*I*4/*mcm*	*Pnma*	*Pm*3*m*	*I*4/*mcm*	*Pnma*
a (Å)	4.11250(5)	5.70251(6)	5.61895(4)	4.12845(8)	5.71068(3)	5.64051(7)
b (Å)		8.05420(16)	7.89309(5)		8.10400(7)	7.9071(1)
c (Å)			5.54878(3)			5.55508(7)
volume (Å^3)	69.553(2)	261.912(3)	246.094(3)	70.366(4)	264.287(4)	247.757(6)
Z	1	4	4	1	4	4
d_{M-X} (Å)[a]	(6×) 2.05625(3)	(2×) 2.01355(4)	(2×) 2.020(8)	(6×) 2.06422(4)	(2×) 2.02600(2)	(2×) 2.016(4)
		(4×) 2.019(5)	(2×) 2.026(2)		(4×) 2.0287(4)	(2×) 2.043(1)
			(2×) 2.033(8)			(2×) 2.045(4)
$\angle_{M-X-M}$ (°)[a]	(3×) 180	(1×) 180	(1×) 153.9(4)	(3×) 180	(1×) 180	(1×) 150.7(3)
		(2×) 173.8(5)	(2×) 153.9(3)		(2×) 168.8(2)	(2×) 154.2(2)

[a] X represents statistically distributed O and N.

Table 2. Rietveld Refinement Details for $SrNbO_2N$ and $CaNbO_2N$, Obtained from Analysis of Cu Kα X-ray Powder Diffraction Data Collected at Room Temperature

formula	$SrNbO_2N$	$CaNbO_2N$
R_{wp}	0.0796	0.0795
$R(F^2)$	0.0614	0.0702
reduced χ^2	8.79	5.70
no. of reflections	72	226
no. of variables	13	21
Z	4	4
crystal system	tetragonal	orthorhombic
space group	*I*4/*mcm*	*Pnma*
a (Å)	5.71068(3)	5.64051(7)
b (Å)	8.10400(7)	7.90711(11)
c (Å)		5.55508(7)
volume (Å^3)	264.287(4)	247.757(6)

Table 3. Atomic Parameters for $SrNbO_2N$ and $CaNbO_2N$

atom	Wyckoff site	*x*	*y*	*z*	U_{iso} (Å^2)
		$SrNbO_2N$			
Sr	4*b*	0	1/2	1/4	0.0113(2)
Nb	4*c*	1/2	1/2	1/2	0.0113(2)
O/N(1)	4*a*	0	0	1/4	0.121(6)
O/N(2)	8*h*	0.7745(4)	0.2745(4)	0	0.121(6)
		$CaNbO_2N$			
Ca	4*c*	0.0350(3)	1/4	−0.0062(6)	0.0167(4)
Nb	4*b*	1/2	0	0	0.0123(2)
O/N(1)	4*c*	0.4763(11)	1/4	0.0899(10)	0.0045(7)
O/N(2)	8*h*	0.2902(6)	0.0420(5)	0.7125(6)	0.0045(7)

mary of the important crystallographic features resulted from these refinements is given in Table 1, and full crystallographic details for $SrNbO_2N$ and $CaNbO_2N$ are shown in Tables 2 and 3, respectively. Because the two anions, O^{2-} and N^{3-}, have indistinguishable X-ray scattering factors no attempt was made in the refinements to differentiate between them. The results for the tantalum oxynitrides are in very good agreement with previous reports in the literature. This agreement not only confirms the fact that our synthetic efforts produce the same compounds as previously reported, but it also validates the relative accuracy of the refined structures of $SrNbO_2N$ and $CaNbO_2N$.

Each of the niobium compounds is found to be isostructural with its tantalum analogue. Interestingly, the niobium compounds consistently have a unit cell volume that is larger than its tantalum analogue by 0.7−1.2%. This result is not expected from the identical ionic radii of the two ions.[24] A possible explanation of this effect may be the introduction of a small concentration of carriers into the conduction band, which would result in partial reduction of Nb^{5+}. The presence of some carriers in the conduction band would also be consistent with the nonnegligible absorbance that the niobium oxynitride samples show at photon energies below the band gap. Another interesting comparison is that between $ANbO_3$ (A = Ba, Sr, Ca) perovskites, containing Nb^{4+}, and the corresponding $ANbO_2N$ oxynitride phases (similar $ATaO_3$ compounds are not known). $BaNbO_3$ and $CaNbO_3$ are isostructural with $BaNbO_2N$ and $CaNbO_2N$, respectively,[25,26] whereas $SrNbO_3$ is orthorhombic with *Pnma* symmetry.[27] Considering the six coordinated ionic radii of Nb^{4+} and Nb^{5+} (0.68 vs 0.64 Å) it is somewhat surprising to find that the $ANbO_3$ compounds have smaller unit cell volumes than their respective $ANbO_2N$ phases. The $ANbO_3$ cell volume is smaller by 2.9%, 1.2%, and 0.1% for A = Ba, Sr, and Ca, respectively. This comparison shows that the average Nb−N distance must be larger than the average Nb−O distance, which is consistent with the four coordinate ionic radii of N^{3-} (1.46 Å) and O^{2-} (1.38 Å). The decreasing difference in the unit cell volume as the size of the alkaline-earth cation decreases is not understood.

The crystal structures of $ANbO_2N$ (A = Sr, Ca) are shown in Figure 2. Octahedral tilting distortions lower the symmetry of the strontium and calcium compounds, but maintain the approximate octahedral environment about the transition metal ion and the corner-sharing connectivity of the perovskite structure. This type of distortion is very common in perovskites of all descriptions.[28,29] Using Glazer's notation[30] to describe the octahedral tilting distortion we can say that the strontium compounds undergo an $a^0a^0c^-$ distortion lowering the symmetry to the tetragonal space group *I*4/*mcm*, while the calcium compounds undergo an $a^-b^+a^-$ distortion lowering the symmetry to the orthorhombic space group *Pnma*. This behavior closely mirrors that of the oxide perovskite analogues $SrTiO_3$ and $CaTiO_3$. $SrTiO_3$ undergoes a transition from *Pm*3*m* to *I*4/*mcm* upon cooling below 110 K,[31] and $CaTiO_3$ adopts the *Pnma* distortion of the perovskite structure at all temperatures

(24) Shannon, R. D. *Acta Crystallogr.* **1976**, *A32*, 751.
(25) Casais, M. T.; Alonso, J. A.; Rasines, I.; Hidalgo, M. A. *Mater. Res. Bull.* **1995**, *30*, 201.
(26) Istomin, S. Ya.; Svensson, G.; D'yachenko, O. G.; Holm, W.; Antipov, E. V. *J. Solid State Chem.* **1998**, *141*, 514.
(27) Hannerz, H.; Istomin, S. Ya.; Svensson, G.; D'yachenko, O. G. *J. Solid State Chem.* **1999**, *147*, 421.
(28) Mitchell, R. H. *Perovskites. Modern and Ancient*; Almaz Press: Thunder Bay, ON, 2002; pp 43−44.
(29) Lufaso, M. W.; Woodward, P. M. *Acta Crystallogr.* **2001**, *B57*, 725.
(30) Glazer, A. M. *Acta Crystallogr.* **1972**, *B28*, 3384.
(31) Shirane, G.; Yamada, Y. *Phys. Rev.* **1969**, *177*, 858.

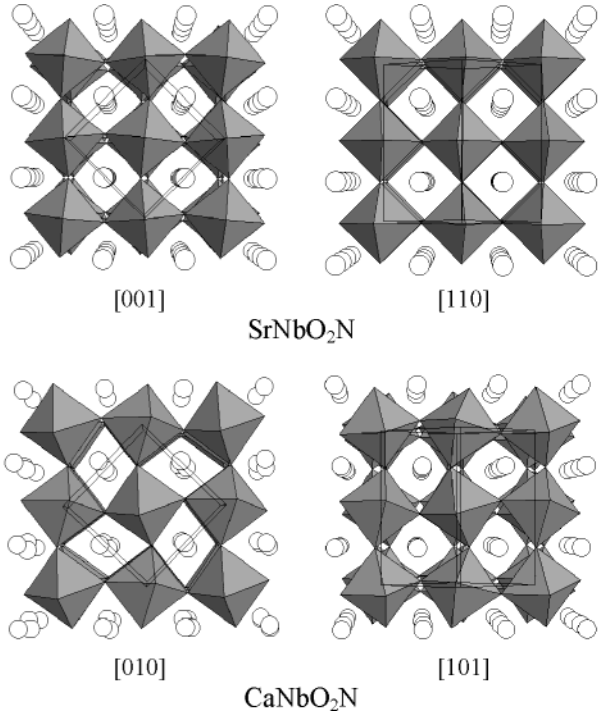

Figure 2. Crystal structures of $SrNbO_2N$ and $CaNbO_2N$ illustrating the octahedral tilting distortions. Sr and Ca are represented with open circles among the corner sharing Nb-$(O,N)_6$ octahedra.

below 1380 K.[32] The comparison with the $ATiO_3$ perovskites breaks down though when A = Ba. $BaTiO_3$ is a well-known and technologically important ferroelectric material. The relationship between ferroelectricity and crystal chemistry in $BaTiO_3$ can be described in simple terms: the large size of the Ba^{2+} ion stretches the titanium-centered octahedra, leading to a displacement of the Ti^{4+} ion from the center of the octahedron toward a face (T < 183 K, space group $R3m$), an edge (183 K < T < 278 K, space group $Bmm2$), or a corner (278 K < T < 393 K, space group $P4mm$) of the octahedron.[28] The tetragonal symmetry and near 180° bond angles of $SrMO_2N$ (M = Ta, Nb) indicate that Sr^{2+} is a good fit (slightly too small) to the octahedral corner-sharing network. Therefore, it is reasonable to expect that one or both of the $BaMO_2N$ compounds would show phase transitions and ferroelectricity similar to $BaTiO_3$. Consideration of the geometric tolerance factors[33] of these compounds also gives rise to the same conclusion. Yet our room-temperature XRPD patterns show no sign of deviation from cubic symmetry, in full agreement with the previous neutron study of Pors et al.[22a] Instead the average Ta−O/N and Nb−O/N distances are significantly elongated from ∼2.02 Å in $SrMO_2N$ to ∼2.06 Å in $BaMO_2N$. Such a dramatic expansion of symmetric octahedra in response to an increase in the size of the A-site cation has no parallel among oxide perovskites.

Variable Temperature X-ray Powder Diffraction. To probe for phase transitions, thermal stability and thermal expansion behavior of all three $ATaO_2N$ phases were examined by variable temperature XRPD in an atmosphere of H_2/Ar (5%/95%). The evolutions of

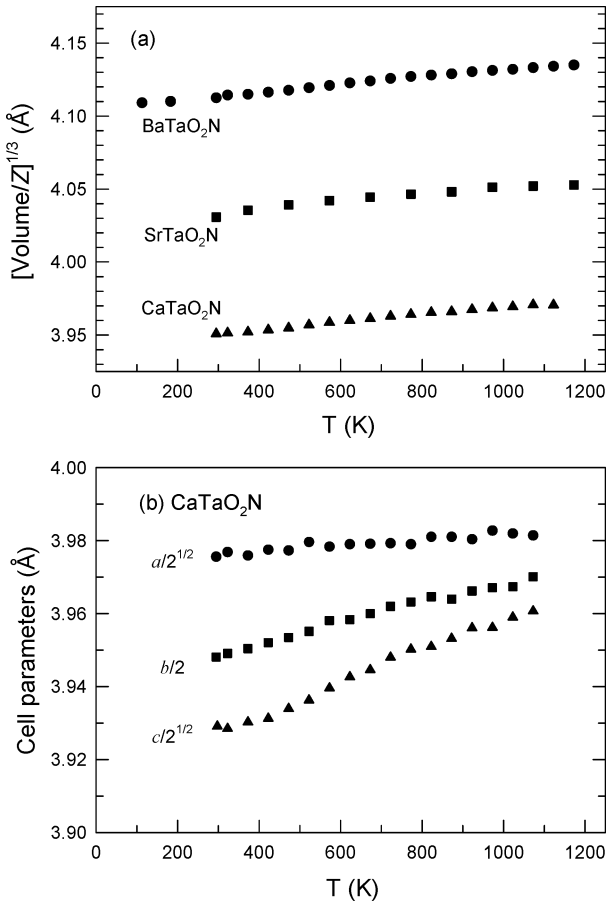

Figure 3. Temperature-dependent unit cell dimensions of $ATaO_2N$ (A = Ba, Sr, Ca) phases as determined by variable temperature XRPD: (a) normalized unit cell edge, (volume/Z)$^{1/3}$, of $BaTaO_2N$, $SrTaO_2N$, and $CaTaO_2N$; and (b) reduced unit cell parameters of $CaTaO_2N$.

the XRPD patterns indicate that all the three phases are stable in this atmosphere up to 1173 K with steady volume increases. The orthorhombic anisotropy of $CaTaO_2N$ gradually decreases, but a transition to tetragonal symmetry does not occur at temperatures below 1173 K. The pseudocubic nature of the $SrTaO_2N$ structure (at room temperature $\sqrt{2}a/c$ = 1.0013) makes detection of the tetragonal distortion difficult. This obscures the exact temperature at which the tetragonal to cubic transition occurs. The transition occurs below 973 K, but, given the subtlety of the tetragonal distortion and the signal-to-noise ratio of the data collected in our high-temperature stage, an exact transition temperature could not be determined in the present investigation. At each temperature of measurement, cell parameters and volumes were determined as presented in Figure 3. Analysis of these data allows us to estimate the mean linear expansion coefficients (α) as 26, 23, and 26 ppm/K for $BaTaO_2N$, $SrTaO_2N$, and $CaTaO_2N$, respectively. Referring to the previously compiled thermal expansion data,[34] the perovskite oxides typically have α values ranging between 5 and 12 ppm/K and typically nitrides have smaller α values than those of isostructural oxides,[35] due to the greater bond strengths

(32) Kennedy, B. J.; Howard, C. J.; Chakoumakos, B. C. *J. Phys.: Condens. Matter* **1999**, *11*, 1479.
(33) Goldschmidt, V. M. *Naturwissenschaften* **1926**, *14*, 477.
(34) (a) Taylor, D. *Br. Ceram. Trans. J.* **1985**, *84*, 181. (b) Henry, J. L.; Thompson, G. G. *Am. Ceram. Soc. Bull.* **1976**, *55*, 281.
(35) Iwanaga, H.; Kunishige, A.; Takeuchi, S. *J. Mater. Sci.* **2000**, *35*, 2451.

and the correspondingly smaller thermal expansion coefficients of those bonds. Therefore, one might expect that the oxynitride perovskites would have lower thermal expansion coefficients than observed. However, it should be noted that changes in octahedral tilting in perovskites provide an additional contribution to the thermal expansion coefficient.[36] In general, thermal expansion reduces the octahedral tilting, and accordingly framework structures with tilted polyhedral linkages always have larger α values than similar structures where tilting is less pronounced. For example, $CaTiO_3$ and $BaTiO_3$ have α's of 25 and 7 ppm/K, respectively, at 273−373 K, and $NaNbO_3$ and $KNbO_3$ have α's of 11 and 5 ppm/K, respectively, at 293−473 K.[36] In fact, these comparisons indicate that the change of tilting has a greater effect on lattice volume than changes in bond length. However, tilting considerations do not explain the large observed α's of $BaTaO_2N$ and $SrTaO_2N$.

Electron Diffraction. The argumentation of the preceding paragraphs suggests the possibility that for one or both of the $BaMO_2N$ compounds the long-range average crystal structure and the local crystal structure may not be the same. Electron diffraction (ED) is known to be a powerful tool for detecting distortions and orderings that are coherent only in small domains. Therefore, ED patterns were collected in transmission mode on $BaTaO_2N$. Figure 4a, b, and c are selected-area diffraction patterns recorded with the electron beam striking the sample along [001], [101], and [113]. The patterns were indexed using a simple $Pm3m$ cubic model for the structure with a lattice constant of 4.1 Å, consistent with the results determined from XRPD data analysis. The appearance of the diffraction patterns is highly reminiscent of diffraction patterns observed for undistorted cubic AMX_3 perovskite ceramics and crystals, in which the (100) reflection is typically weak compared to the (200) reflection at [100] zone axis. The weak intensity of the (100) reflection follows directly from structure factor considerations when the electron densities on the A and M sites are similar. Exhaustive study of several grains of $BaTaO_2N$ did not reveal any evidence for long-range structural ordering, which could be detected by the presence of various superstructure reflections. A number of grains were studied along various high-order zone-axes to observe diffuse scattering that might indicate short-range ordering, displacive relaxation, and/or a lowering of the symmetry. All the diffraction patterns were seen to be free from diffuse scattering. Therefore, it can be deduced that if any cooperative distortions from cubic symmetry do take place they must occur within sub-nanometer domains. This observation strongly supports a model where the O/N distribution in $BaTaO_2N$ is disordered and maintains a virtually perfect 2:1 ratio.

Dielectric and Electrical Transport Properties. Although the d^0 transition metal oxynitride perovskites have been known for some time, there has been very little investigation of their dielectric or electrical transport properties. This can probably be attributed to the difficulty in obtaining either single crystals or sintered pellets of these materials. As described in the Experimental Section we were able to produce sintered pellets by cold isostatic pressing followed by an additional heat treatment in flowing NH_3 at 1293 K. Although far from the conventional ceramic sintering procedure, sintering in air or in a vacuum would lead to decomposition of the samples, and was not an option. Furthermore, the final heat treatment in the sintering process was found to be essential to obtain meaningful measurements of the electrical properties. After heating, both $BaTaO_2N$ and $SrTaO_2N$ pellets remained intact and their coloration showed minimal changes, but the other samples did display some signs of change. The bright yellow $CaTaO_2N$ became slightly darkened and $BaNbO_2N$

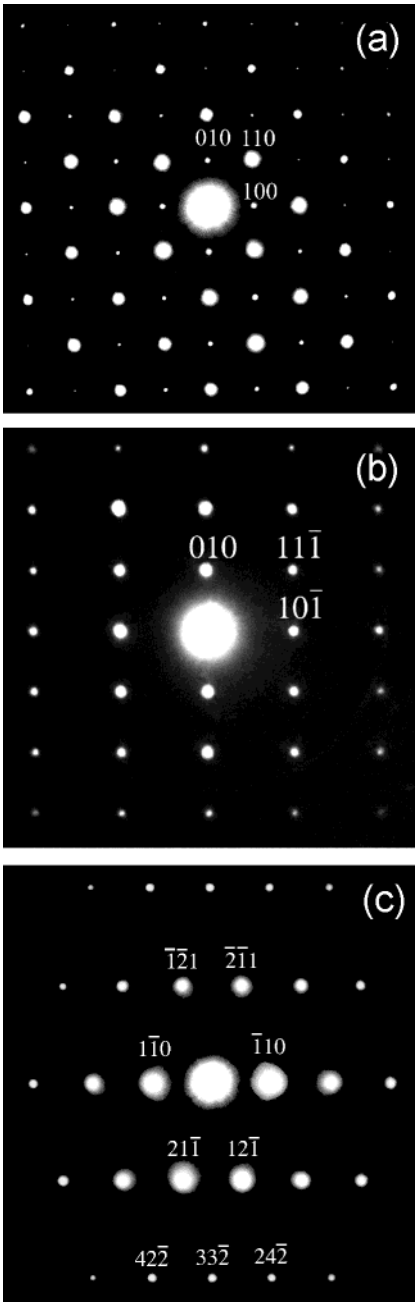

Figure 4. Selected-area electron diffraction patterns recorded in the TEM from crystallites of $BaTaO_2N$ along (a) [100], (b) [101], and (c) [113], respectively. The diffraction patterns are consistent with a simple perovskite structure with a weak (100) and strong (200) reflections along [100]. There is no evidence of any superstructure reflections or diffuse scattering in the diffraction patterns.

(36) Megaw, H. D. *Mater. Res. Bull.* **1971**, *6*, 1007.

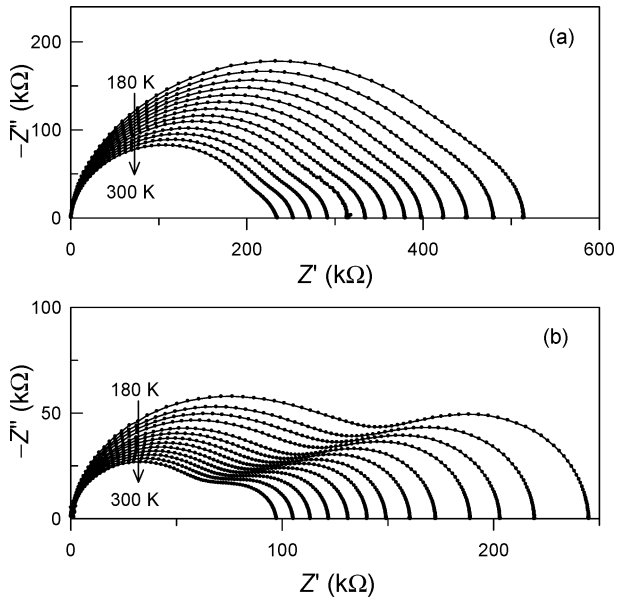

Figure 5. Temperature-dependent impedance spectra for (a) $BaTaO_2N$ and (b) $SrTaO_2N$, measured at 180−300 K and at $1-10^7$ Hz.

turned from dark brown to gray black. However, careful XRPD investigations indicated that even the latter two compounds maintain essentially the same crystal structures without the appearance of any noticeable impurities. XRPD patterns and UV−Visible absorption plots for $BaNbO_2N$, before and after the heat treatment, are given in the Supporting Information. Although the pellets still showed considerable porosity (∼45% porosity), the sintering of grains was sufficient to give mechanical strength and electrical conductivity pathways necessary for characterization. Unfortunately, for $SrNbO_2N$ and $CaNbO_2N$, heating caused severe deformations of pellets together with color changes (the pellets became lighter), so that they were not suitable for further characterization.

Electrical conductivities and dielectric permittivities of $BaTaO_2N$, $SrTaO_2N$, $CaTaO_2N$, and $BaNbO_2N$ have been evaluated by ac impedance analysis over the temperature range 180−300 K and the frequency range $1-10^7$ Hz. The measured impedance spectra for $BaTaO_2N$ and $SrTaO_2N$ were composed of two semicircles representing the bulk and grain boundary contributions (see Figure 5). For the nonlinear curve fitting of the spectra a corresponding equivalent circuit model was used, where each of two serial components (one representing the bulk and one the grain boundaries) was taken as a resistor and a constant phase element[19] in parallel.

The apparent permittivities of the ceramic pellets, in which the bulk and grain boundary contributions are convoluted, are shown in Figure 6 as a function of temperature for several frequencies. The extracted values for the bulk and grain boundary permittivity and electrical conductivity at room temperature are given in Table 4. Figure 7a shows the bulk electrical conductivities, σ_{el}, of $BaTaO_2N$ and $SrTaO_2N$ in the temperature range between 180 and 300 K. Both compounds are poor electrical conductors, $\sigma_{el} \approx 10^{-5}$ S/cm, exhibiting activated transport behavior. From the Arrhenius plots the activation energies are estimated to be 0.010 eV for $BaTaO_2N$ and 0.013 eV for $SrTaO_2N$. The relatively small activation energies suggest that the insulating behavior arises from very low carrier concentrations. Although these compounds are not good electrical conductors, they do show conductivities that are higher than those of typical oxides containing Ta^{5+} by several orders of magnitude. This is not unexpected in light of the large reduction in band gap that ac-

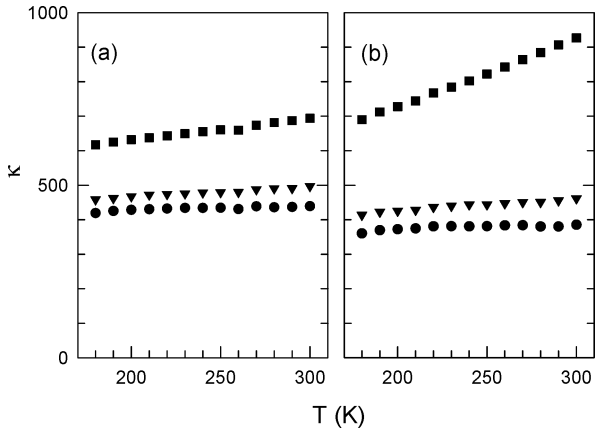

Figure 6. As-measured relative permittivities of (a) $BaTaO_2N$ and (b) $SrTaO_2N$ samples as functions of temperature at selected frequencies, 10 kHz (filled squares), 100 kHz (filled inverted triangles), and 1 MHz (filled circles). Data represent the combined bulk and grain boundary contributions.

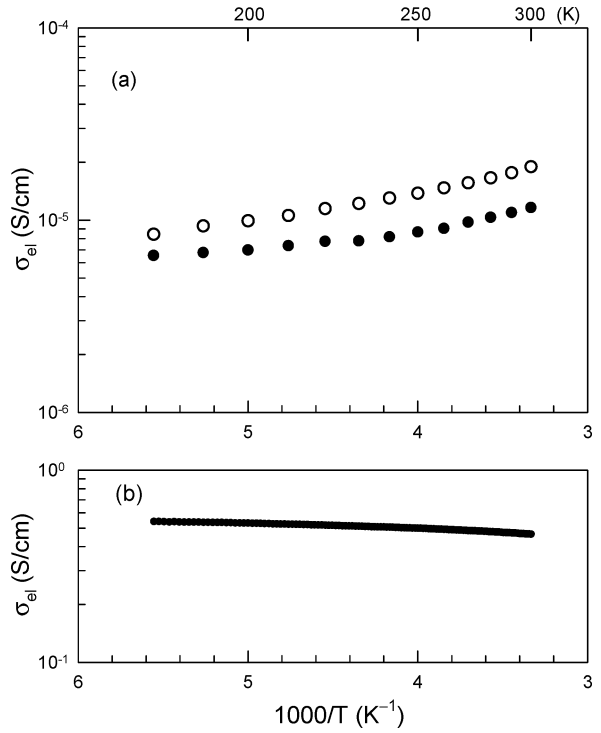

Figure 7. Arrhenius plot of electrical conductivities for (a) $BaTaO_2N$ (filled circles) and $SrTaO_2N$ (open circles), and (b) $BaNbO_2N$ in the range of 180−300 K. For all data points, error bars lie within the symbols.

Table 4. Relative Permittivities and Conductivities of Bulk and Grain Boundary Components in $BaTaO_2N$ and $SrTaO_2N$ Ceramics at Room Temperature

	bulk		grain boundary	
	σ_{el} (S/cm)	κ	σ_{el} (S/cm)	κ
$BaTaO_2N$	1.1×10^{-5}	4870	3.3×10^{-5}	3.21×10^5
$SrTaO_2N$	1.8×10^{-5}	2870	2.9×10^{-5}	1.31×10^5

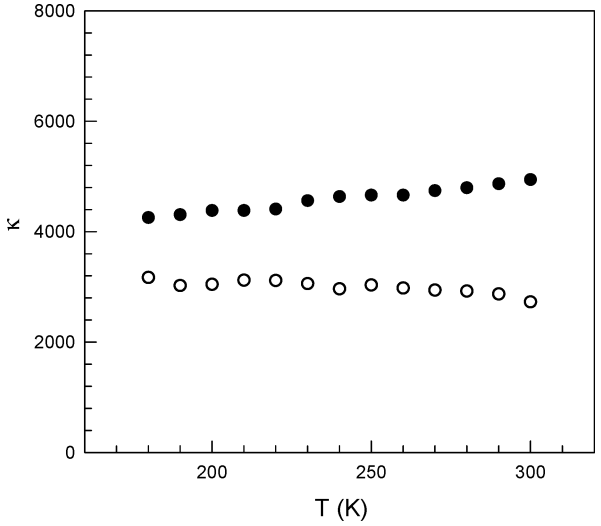

Figure 8. Temperature-dependent relative permittivities of bulk $BaTaO_2N$ (filled circles) and SrTaO2N (open circles) at 180−300 K, obtained from analysis of impedance spectra. For all data points, error bars lie within the symbols.

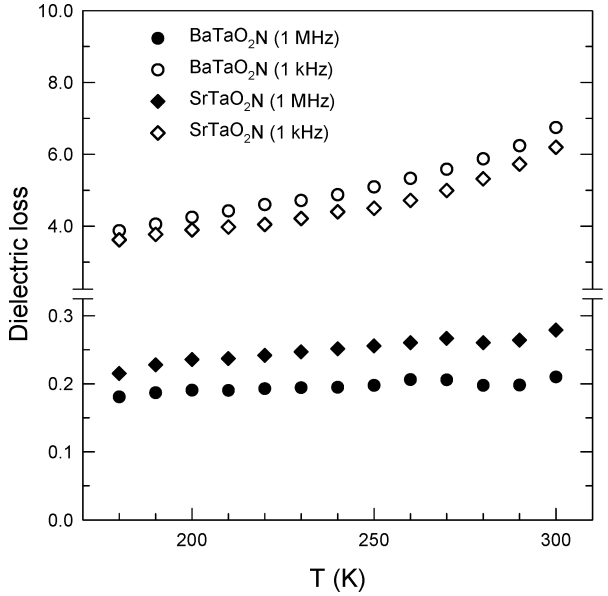

Figure 9. Dielectric loss for $BaTaO_2N$ and $SrTaO_2N$ at 1 MHz and 1 kHz.

companies partial replacement of O^{-2} with N^{-3} (1.8 eV in $BaTaO_2N$, 2.1 eV in $SrTaO_2N$, vs 3.5 eV in $KTaO_3$).

In Figure 8, the temperature-dependent bulk permittivity, κ, of $BaTaO_2N$ and $SrTaO_2N$ are plotted as obtained from the equivalent circuit analysis. Both compounds are found to possess very high κ values on the order of 3000−5000. The high dielectric permittivities of these two compounds are reminiscent of the values seen in $BaTiO_3$. It is noteworthy that the ferroelectric-like high κ's of present dielectric systems show only moderate temperature dependences over the range of study. For $BaTaO_2N$ and $SrTaO_2N$, the temperature coefficients of κ (tcκ) are calculated as +1140 and −730 ppm/K, respectively. These values are larger than those of medium κ dielectrics (κ < 100 and tc$\kappa \approx$ 10 ppm/K) but are smaller than those of ferroelectrics. Furthermore, the opposite signs of the $BaTaO_2N$ and $SrTaO_2N$ tcκ values offers the tantalizing possibility that solid solutions could be formed with high permittivity and near-zero temperature dependence. The dielectric behaviors of these oxynitrides are distinguished even from those of relaxors that still retain a trace of the ferroelectric phase transition. Keep in mind that for cubic $BaTaO_2N$ no phase transition is likely to occur up to its decomposition temperature, while for $SrTaO_2N$ a tetragonal-to-cubic transformation is a possibility, but the impact on the dielectric constant is likely to be minor.

Figure 9 shows the dielectric loss for $BaTaO_2N$ and $SrTaO_2N$, measured at 1 kHz and 1 MHz. For both compounds the temperature and frequency dependences of loss are quite similar to those of κ shown in Figure 6, smoothly getting larger at higher temperature and at lower frequency. At 1 MHz the dielectric loss of $BaTaO_2N$ and $SrTaO_2N$ are ∼0.2, several orders higher than the desired level for practical applications. At these frequencies dielectric loss, or the dissipation of electric potential, is generally attributed to heat generation at lattice defects and electrical conduction within the crystal. Simple formalism of dielectric loss for a circuit composed of a resistor and a capacitor in parallel, $\tan \delta = -Z'/Z'' = 1/(\omega RC)$, shows that a low dielectric loss can be obtained only when a solid possesses both high resistance and capacitance, let alone very low defect concentration. In the present compounds, the intrinsic component of the loss likely originates in the electrical conduction process, but the low packing density of the sample specimen undoubtedly provides a significant external contribution to the dielectric loss. The conductivity of $\sim 10^{-5}$ S/cm in these two compounds may set the lower limit for the loss term. However, it is quite possible that most of the contribution to the loss in these measurements can be traced to extrinsic sources associated with the relatively high porosity of the sintered pellets. It is expected that the loss will decrease significantly as sample sintering improves and the measurement frequency increases.

The electrical properties of $CaTaO_2N$ and $BaNbO_2N$ are markedly different from the high-κ behavior of the previous two compounds, and very distinctive from each other. Separation of the bulk and grain boundary contributions was not possible with either compound, due to the highly insulating nature of $CaTaO_2N$ and the highly conducting nature of $BaNbO_2N$. $CaTaO_2N$ is not only a poorer electrical conductor, $\sigma_{el} \approx 10^{-8}$ S/cm, than $ATaO_2N$ (A = Ba, Sr), its relative permittivity is dramatically lower, taking on a value $\kappa \approx 30$. This value is fairly typical for an insulating perovskite oxide. At the other extreme, the resistivity of $BaNbO_2N$ is smaller by 7 orders of magnitude, σ_{el} of $\sim 10^{-1}$ S/cm, and decreases as the temperature decreases, as represented in Figure 7b. The high σ_{el} and its metallic-type temperature dependence are wildly different from its tantalum counterparts. This behavior most likely originates from partial $Nb^{5+} \rightarrow Nb^{4+}$ reduction, a process that would lead to the introduction of carriers into the conduction band. The nonnegligible optical absorbance at energies below the band gap (see Figure 1) is suggestive of such doping, and it was noted above that the color darkens to gray-black upon the final sintering treatment, implying further doping. The covalency of the Nb−O/N interaction should be sufficient to allow for delocalized carrier transport once carriers are introduced through doping. As a point of comparison consider the fact that

$BaNbO_3$ is a Pauli paramagnetic conductor, and the replacement of oxide ions with nitride ions will only further increase the covalency.[25] It must be noted that during synthesis of the niobium compounds a competing secondary phase is niobium oxynitride, NbO_xN_y, which contains reduced niobium and is itself a good electrical conductor.[37] This raises the possibility that the conductivity originates in an impurity phase, rather than the $BaNbO_2N$ phase itself. Considering the intermediate observations during $ANbO_2N$ syntheses where NbO_xN_y formation occurred at the surface, NbO_xN_y formation in the pellet specimen would be pronounced at surface layer. However, the sintered $BaNbO_2N$ pellet had a uniform color across its thickness, and measurements of its conductivity using freshly polished surfaces were very reproducible. Moreover, an inspection by XRPD revealed no discernible change in the diffraction pattern as a result of sintering, with no signs of niobium oxynitride. Therefore, it is unlikely that a NbO_xN_y is responsible for the observed conductivity, and we believe that the conductivity originates from the presence of free charge carriers in $BaNbO_2N$. It is interesting to note that high electronic conductivity in response to low doping levels is atypical behavior for oxide perovskites, due to electron correlation effects. Clearly this compound merits further study.

Discussion

Ferroelectricity in d^0 transition metal oxide perovskites, such as $BaTiO_3$, $PbTiO_3$, and $KNbO_3$ is well established. It is not so common in oxides containing Ta^{5+} because of the reduced electronegativity of this ion in comparison to its neighbors Nb^{5+} and Ti^{4+}, and the corresponding decrease in the covalency of the metal−oxygen interaction. However, the presence of N^{-3}, which is less electronegative than O^{-2}, acts as a compensating mechanism that may enable displacements of Ta^{5+} ions, which would in turn give rise to a high dielectric permittivity. A truly centrosymmetric crystal cannot exhibit a permanent nonzero dipole moment because all the local dipoles will be counterbalanced by each other within the unit cell. Accordingly, it is hard to reconcile the nonpolar point group symmetries of $BaTaO_2N$ and $SrTaO_2N$ with the very high κ values observed. To understand these seemingly conflicting results, it is necessary to carefully consider the local structures of AMO_2N oxynitrides with respect to the O/N ordering. Assuming that each M^{5+} ion in the above oxynitrides is coordinated with four oxygens and two nitrogens, there can be cis- and trans- isomers of MO_4N_2 octahedra. A recent computational study by Fang et al. based on first principles density-functional theory examined the energetics and structure of various ordered and disordered models of $BaTaO_2N$.[38] They found that in both cis- and trans- ordered models each Ta^{5+} ion shifts by ~0.1 Å from its high symmetry position at the center of the octahedron. They did not comment directly on the nature of the shift in the cis- isomer, but presumably it is toward the nitride-rich edge of the octahedron. The shift of the Ta in the trans- isomer gives rise to a short Ta−N bond of 1.89 Å and a long Ta−N bond of 2.33 Å. Furthermore, their calculations suggest that there is very little energetic difference between either of the two ordered models, and a disordered anion arrangement. Thus, when the entropy is taken into account, a disordered O/N distribution is expected to be the most stable configuration.

The implications of the computational study of Fang and co-workers are interesting and relevant to the dielectric properties of these compounds. Most importantly both cis- and trans- isomers are predicted to form polar octahedral units, so that in a perfectly ordered compound either ferroelectric or antiferroelectric behavior is expected. In the presence of a partially ordered, or as appears to be the case here, a disordered anion arrangement the long range order of the Ta displacements will be lost and relaxor-type behavior is expected. Their calculations did not address the effects of substituting strontium or calcium for barium. Upon going from $BaTaO_2N$ to $SrTaO_2N$ the stretching of the octahedra is lost, but only a minimal octahedral tilting distortion is observed. By analogy with $BaTiO_3$ and $SrTiO_3$ one might expect that such a substitution would dampen any displacements of the Ta ions and dramatically lower the dielectric constant. While it is true that at room temperature the measured permittivity of $BaTaO_2N$ is almost twice that of $SrTaO_2N$, the dielectric constant of the strontium compound is still very high. The reason for this may lie in the covalency of the Ta−N bonds, and the nonequivalent identity of the six anions surrounding each tantalum ion. It would seem that these features allow Ta displacements even when the octahedra are allowed to relax their normal size. A better analogy may lie in the crystal chemistry of $KNbO_3$ and $NaNbO_3$. $KNbO_3$ is a ferroelectric, with a tolerance factor larger than unity. Its crystal chemistry and dielectric properties are similar in many ways to those of $BaTiO_3$. In $NaNbO_3$ simple tolerance factor considerations suggest that the niobium atoms should remain at the center of each octahedron, but instead the covalency of the Nb−O bonding leads to out-of-center displacements of the Nb atoms in combination with octahedral tilting distortions.[39] Similar behavior occurs for similar reasons in WO_3.[40] Interestingly, our measurements suggest that $CaTaO_2N$ does not have a large dielectric constant like the Ba and Sr analogues. One possible explanation is that the significant increase in the octahedral tilting distortion quenches the out-of-center displacements of the tantalum ions, or alters the anion distribution. Another possibility is that the dramatic change in the dielectric properties upon replacing Sr with Ca is not an intrinsic property, but stems from the lack of sintering and grain growth in the calcium analogue. Further studies are needed to unequivocally determine whether the dielectric properties of $CaTaO_2N$ are distinct or similar to the strontium and barium analogues.

It has been established that the tantalum oxynitride perovskites are quite stable in air, water, or even in

(37) Petrenko, S. V.; Protsenko, I. E.; Smolin, M. D. *Izv. Vyssh. Uchebn. Zaved., Fiz.* **1986**, *29*, 90.

(38) Fang, C. M.; de Wijs, G. A.; Orhan, E.; de With, G.; de Groot, R. A.; Hintzen, H. T.; Marchand, R. *J. Phys. Chem. Solids* **2003**, *64*, 281.

(39) Lefkowitz, I.; Lukaszewicz, K.; Megaw, H. D. *Acta Crystallogr.* **1966**, *20*, 670.

(40) (a) Vogt, T.; Woodward, P. M.; Hunter, B. A. *J. Solid State Chem.* **1999**, *144*, 209. (b) Woodward, P. M.; Sleight A. W.; Vogt, T. *J. Solid State Chem.* **1997**, *131*, 9.

strongly acidic solutions. This has been attributed to the formation of an oxide-rich surface around each crystallite. The picture of semiconducting oxynitride crystals encapsulated within an insulating oxide surface suggests the possibility that the high dielectric constants of $BaTaO_2N$ and $SrTaO_2N$ can be attributed to an internal barrier layer capacitor mechanism, similar to what has been proposed for the fascinating dielectric properties of the centrosymmetric compound $CaCu_3Ti_4O_{12}$.[41,42] However, we feel this is not the case with the oxynitrides because the impedance analysis clearly shows high permittivity and high resistivity for both the bulk and the grain boundaries. Thus, the mechanism invoked to explain the properties of $CaCu_3Ti_4O_{12}$ would not seem to be applicable here.

Conclusions

The compounds $BaTaO_2N$ and $SrTaO_2N$ exhibit unusual dielectric properties. Both compounds have bulk permittivities in excess of 2500. They show no traces of phase transitions upon cooling from room temperature, and compared to conventional ferroelectrics the permittivity shows a weak dependence upon temperature. The opposite signs of their tcκ values offer the possibility that solid solutions could be formed with high κ that have near-zero temperature dependence. Once formed, these compounds are very stable in the presence of air, moisture, acids, etc., providing the possibility for technological applications. However, most significantly, it remains a challenge to prepare dense, well-sintered specimens for application and more definitive characterization. One route to realization of this goal may be deposition of thin films of these compounds on a suitable substrate. We are currently investigating this possibility. The fascinating dielectric properties of $BaTaO_2N$ are lost upon replacing Ta with Nb, because the niobium ion is too easily reduced. This reduction actually causes $BaNbO_2N$ to be a very good electrical conductor. The small temperature dependence of the electrical conductivity of this latter compound suggests it is a heavily doped, degenerate, semiconductor.

Acknowledgment. Financial support for this research was provided by the National Science Foundation, grant DMR-0094271.

Supporting Information Available: Rietveld refinement profiles for XRPD patterns of AMO_2N; XRPD patterns of $BaNbO_2N$, $BaTaO_2N$, and $SrTaO_2N$, collected before and after the sample processing for electrical measurements; diffuse reflection−absorption spectra of $BaNbO_2N$ recorded before and after the sample processing for electrical measurements (PDF). This material is available free of charge via the Internet at http://pubs.acs.org.

CM034756J

(41) Subramanian, M. A.; Dong, L.; Duan, N.; Reisner, B. A.; Sleight, A. W. *J. Solid State Chem.* **2000**, *151*, 323.
(42) Sinclair, D. C.; Adams, T. B.; Morrison, F. D.; West, A. R. *Appl. Phys. Lett.* **2002**, *80*, 2153.